16th World Conference on Earthquake, 16WCEE 2017

Santiago Chile, January 9th to 13th 2017

Paper N° 1732

Registration Code: S-T1464293744

Experimental Testing of Partially Bonded Fiber-Reinforced Elastomeric Isolators

N.C. Van Engelen [(1)], M.J. Tait [(2)], D. Konstantinidis[(3)]

[(1)] *Project Scientist, Rowan Williams Davies & Irwin Inc., Niel.VanEngelen@RWDI.com*
[(2)] *Professor, McMaster University, taitm@mcmaster.ca*
[(3)] *Assistant Professor, McMaster University, konstant@mcmaster.ca*

Abstract

Originally presented as a low-cost alternative, Fiber-Reinforced Elastomeric Isolators (FREIs) have been shown to achieve similar performance as conventional steel-reinforced elastomeric isolator designs. A component of the cost reduction centred on positioning the isolator unbonded between the upper and lower supports, eliminating the need for large steel end plates and bonding procedures. Unbonded FREIs exhibit a unique deformed shape, known as *rollover*. Rollover is associated with a reduction in the effective lateral stiffness (lateral softening) as the isolator is displaced; an advantageous feature to increase the efficiency of the isolation system that also allows for adaptive design. Although the unbonded application is a necessity for rollover to occur, it is also attributed to perceived limitations. Notably, unbonded FREIs rely solely on friction to transfer the lateral force, which may allow slip in certain loading conditions, and does not allow for the transfer of vertical tensile forces. It has been proposed that these concerns can be alleviated by partially bonding the isolator to the supports, thereby forming a hybrid between an unbonded isolator and a conventional fully bonded isolator. This concept, known as Partially Bonded Fiber-Reinforced Elastomeric Isolators (PB-FREIs), merges the beneficial characteristics of both types of isolators to prevent slip, transfers a vertical tensile force, and retains the desirable lateral softening due to rollover. The concept of PB-FREIs is discussed and new experimental and numerical findings are presented to bring further depth to the concept.

Keywords: base isolation; partially bonded; fiber-reinforced; elastomeric isolator

1. Introduction

Steel-reinforced elastomeric isolators (SREIs) have been widely applied in base isolation applications to high importance and post-disaster structures [1]; however, the cost and weight of SREIs has been perceived as barriers to widespread base isolation application. Fiber-reinforced elastomeric isolators (FREIs) were initially proposed as a low-cost base isolation system to address the perceived cost and weight limitations, particularly in developed countries where the devastation due to earthquakes is often more severe [2]. The concept of FREIs requires the replacement of the steel reinforcing shims with fiber reinforcement that has comparable tensile mechanical properties, and the removal of the large steel endplates used to mechanically fasten the isolator to the upper and lower supports. By eliminating the steel components, it was proposed that FREIs could be manufactured in large pads and subsequently cut to the desired size [2].

A subsequent experimental investigation identified that unbonded FREIs could exhibit advantageous lateral softening and stiffening adaptive characteristics [3]. Although initially intended as a cost saving measure, the unbonded installation, combined with the lack of flexural rigidity of the fiber reinforcement, results in a unique deformation during lateral displacement, denoted as *rollover*. Rollover occurs as the initially lateral surfaces of the isolator lose contact with the upper and lower supports, forming a curved rollover section, identified in Fig. 1(a). Rollover is the cause of the softening in unbonded FREIs. Rollover will continue with increasing lateral displacement until *full rollover* occurs, illustrated in Fig. 1(b). Full rollover is the full contact of the initially vertical faces of the isolator to the lateral supports. Full rollover prevents further rollover from occurring, thereby stiffening the isolator with increasing lateral displacement. The retention of a positive tangential stiffness (i.e. lateral stability) is determined by the width-to-total height aspect ratio of the isolator. Isolators that maintain lateral stability while demonstrating these adaptive characteristics have been denoted as stable unbonded FREIs (SU-FREIs) [4].

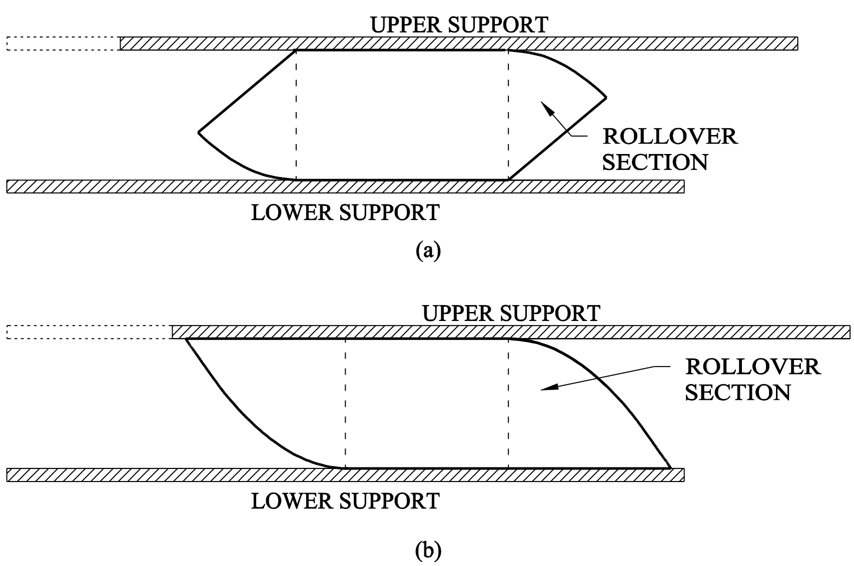

Fig. 1 – (a) Rollover and (b) full rollover of an unbonded FREI

The unbonded application of FREIs, although in part responsible for the adaptive characteristics, is also the source for two potential limitations: susceptibility to slip and subsequent residual displacements, and the inability to transfer tensile forces that may occur under certain loading conditions. Van Engelen et al. [5] proposed that these potential limitations could be addressed by partially bonding the bearing to steel endplates, which could be mechanically fastened to the upper and lower supports. The resulting isolator, denoted as a partially bonded FREI (PB-FREI), formed a hybrid between a fully bonded and unbonded isolator, merging beneficial features from each isolator, such as the adaptive characteristics and resistance to slip and residual displacements.

The experimental program presented in Van Engelen et al. [5] exclusively investigated the performance of the isolator under compression. In this paper, experimental testing is conducted to investigate the performance of PB-FREIs with a nominal vertical tensile load. A partially bonded isolator with a nominal tensile load is evaluated against an unbonded isolator with a compressive stress. The performance is evaluated based on the effective lateral stiffness and the equivalent viscous damping. It is demonstrated that a PB-FREI can achieve similar performance with a nominal vertical tensile load as with a vertical compressive load.

2. Background

2.1 Fiber-Reinforced Elastomeric Isolators

Steel or fiber reinforcement is necessary to stiffen the vertical properties of the elastomeric isolator, resulting in a device with a high vertical stiffness and low lateral stiffness. As an isolator is compressed, the near-incompressible elastomer bulges laterally to accommodate the vertical compressive strain. The reinforcement restrains the lateral bulging, thus the vertical deflection must be accommodated through volumetric strain, which is related to the bulk modulus. The bulk modulus of elastomers is several orders of magnitude larger than the elastic modulus or shear modulus. The increased dependency on the bulk modulus and volumetric strain can be represented by the shape factor, or the ratio of the loaded plan area to the unloaded perimeter of a single layer of elastomer. Isolators with low shape factors (i.e. thick elastomeric layers) have minimal lateral bulging restraint. As the shape factor increases (i.e. thin elastomeric layers), the layers are restrained, and the compression and bending modulus will theoretically approach the bulk modulus as the shape factor approaches infinity.

The primary analytical difference between a FREI and SREI is that the fiber reinforcement is assumed flexible and extensible, whereas the steel reinforcement is often assumed rigid and inextensible. Analytical solutions for the compression and bending modulus, developed based on the assumptions of the *pressure solution,* including the compressibility of the elastomer and the extensibility of the reinforcement are available for most common pad geometries [6-10]. These solutions demonstrate that, similar to the compressibility of the elastomer, the extensibility of the reinforcement may have a pronounced influence on critical isolator properties. An increase in compressibility (i.e. decrease in bulk modulus) causes an increase in volumetric strain under equal vertical stress, reducing the benefit of the restraint provided by the reinforcement. Similarly, extensible reinforcement also reduces the restraint on the lateral bulging as the reinforcement strains laterally. Although a higher vertical stiffness is generally more desirable, in some contexts, such as vibration isolation, the extensibility of the reinforcement could be used to obtain a desired vertical stiffness that may not be easily achievable with steel reinforcement [11].

FREIs have been experimentally investigated in bonded [12-14] and unbonded [3, 15-20] applications. The unbonded application, in addition to reducing the weight by eliminating the steel endplates, also serves to mitigate the development of tensile stresses in the ends of the isolator, as demonstrated in finite element investigations [20, 21]. A variety of weaves and material types have been investigated for the fiber reinforcement [14, 19, 22]. The selection of different fiber material and weaves is considered beneficial to give a designer increased flexibility to tailor the design of the isolator. Early experimental investigations identified additional energy dissipation may occur in FREIs, which was attributed to the inter-fiber movements [2]; however, an experimental program comparing FREIs and SREIs suggested that the damping was primarily provided by the elastomer [14]. It is postulated that the contribution is a function of the degree of saturation of the fiber reinforcement (i.e. the ability of the fibers to move against one another).

The lateral resistance of the rollover section (which is proportional to the lateral displacement) is less than an equivalent volume of elastomer in simple shear. Thus, as lateral displacement occurs and the size and volume of the rollover section increases, the isolator softens, until full rollover occurs. When full rollover is reached the lateral resistance increases (i.e. the isolator hardens). These adaptive characteristics were identified by Toopchi-Nezhad et al. [3]. In isolators with a low width-to-total height aspect ratio, *R*, the volume of the elastomer that experiences rollover is large relative to the total volume of the elastomer. In these isolators, the softening is substantial and the isolator may become laterally unstable before full rollover occurs. The transition from a laterally unstable to laterally stable isolator occurs at a width-to-total height aspect ratio of approximately 2.5, depending on the layer design [3, 23]. Conversely, if the aspect ratio becomes very large, approximately 10 and greater, the volume of the elastomer that experiences rollover is small in comparison to the total volume of the isolator and the amount of softening becomes negligible. Note that the magnitude and benefits of the softening after $R = 2.5$ decreases with increasing R. Fig. 2 compares the idealized response of an unstable, stable and large aspect ratio isolator.

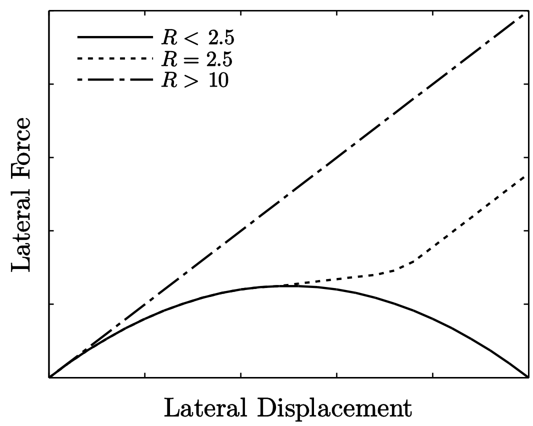

Fig. 2 – Idealized lateral force-displacement relationships of unbonded FREIs based on width-to-total height aspect ratio, R

2.2 Partially Bonded Fiber-Reinforced Elastomeric Isolators

Van Engelen et al. [5] identified that unbonded FREIs with $R > 3.3$ will retain an area that remains in contact with the upper and lower supports regardless of rollover, illustrated in Fig. 3. It was proposed that this area could be bonded to prevent slip and introduce vertical tensile resistance without influencing rollover or full rollover. The resulting isolator was a hybrid of unbonded FREIs and bonded FREIs, retaining the benefits of rollover and full rollover. PB-FREIs require the re-introduction of steel end plates, which contributes to the weight and cost, but addresses the perceived limitations of slip and residual displacement, and vertical tensile resistance.

Van Engelen et al. [5] showed that B_{max}, defined as the maximum ratio of bonded length to total length, a, that could be applied to the center of the bearing without entering the rollover section, can be expressed as:

$$B_{\max} = \left(1 - \frac{10}{3R}\right) \quad (1)$$

Equation (1) was derived from the full rollover prediction presented in Kelly and Konstantinidis [24]. Russo et al. [19] identified that the vertical deflection of the bearing could delay the loss of contact of the elastomer with the supports due to rollover. This was observed in Van Engelen et al. [5] to allow a larger bond length to be applied without influencing the lateral hysteresis loops of the isolator, thus Eq. (1) was considered a conservative lower estimate, and in practice larger bond lengths could be utilized.

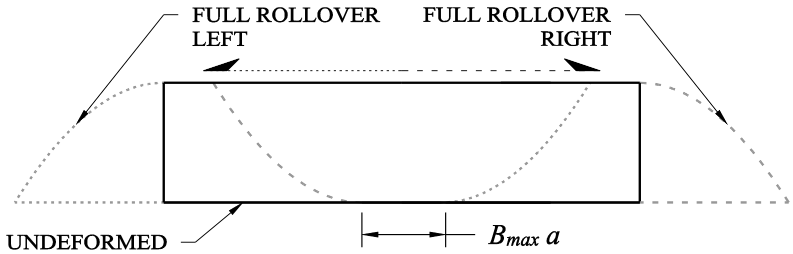

Fig. 3 – Illustration of B_{max}, the theoretical maximum ratio that can be bonded without influencing rollover

The concept of PB-FREIs was validated with an experimental program that compared two FREI designs in partially bonded and unbonded configurations. The cyclic lateral tests, conducted under a vertical compressive load, were used to evaluate a finite element model, which was subsequently used to investigate the vertical tensile modulus and lateral force-displacement relationship with a vertical tensile and compressive load. With a vertical compressive load, the study identified that the partial bond could have a pronounced effect on the lateral force-displacement relationship if the bonded entered the rollover section, forming a bonded rollover section, as illustrated in Fig. 4. The bonded rollover section, similar to the occurrence of full rollover, prevents additional softening and delays (or prevents) full rollover. The results of the finite element investigation suggested that the lateral force-displacement relationship obtained with a vertical tensile load would exhibit similar adaptive characteristics as with a vertical compressive load.

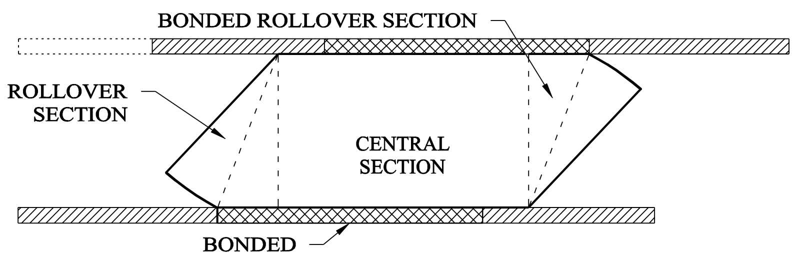

Fig. 4 – Bonded rollover sections introduced due to the partial bond

The introduction of tensile resistance through the partial bond determines that tensile stresses within the elastomer become critical in comparison to an unbonded FREI, which is generally dominated by compressive stresses [21]. Cavitation is a concern when considering tension in elastomeric isolators. The elastomer is susceptible to cavitation at very low tensile strains under the state of tri-axial stress generated by pure tension, although, under combined tension and shear, this damaging effect can be avoided [1]. Theoretical analysis [25] and finite element analysis [1] has found that elastomeric isolators may also buckle in tension, although cavitation is expected to occur before buckling. An experimental investigation [27] confirmed that cavitation can be expected to occur at a stress that is approximately three times the shear modulus. The study also found that isolators that have experienced cavitation can still retain similar performance as prior to cavitation, within certain compressive stresses and shear strain limits.

Investigations on FREIs are almost exclusive to vertical compressive stress since the isolator is usually unbonded. If a vertical compressive load is applied to a multilayer elastomeric isolator at zero lateral displacement, in-plane tensile stresses develop in the fiber reinforcement as the outward lateral bulging of the elastomer is restrained. If a vertical tensile load is applied, the reinforcement may restrain the elastomer from bulging inwards, having a similar overall effect. Fiber reinforcement as a homogeneous material, unlike steel, provides no appreciable resistance in compression. The performance of fiber reinforcement with an in-plane compressive stress as a composite with the elastomeric layers, however, has not been investigated.

3. Experimental Program

3.1 Isolator Design and Bonding

The experimental program consisted of two FREI specimens, shown in Fig. 5. The specimens considered in this investigation were quarter scale and had a similar elastomeric layer design as previous investigations [5, 26]. The specimens had seven layers of Shore A 40 Durometer natural rubber. The two exterior layers of elastomer (i.e. the layers in contact with the upper and lower supports) were half the thickness of the interior layers. The reinforcement, shown in Fig. 6, was plain-weave bidirectional carbon fiber with a nominal thickness of 0.25 mm. The total thickness of the elastomeric layers, t_r, was 19.1 mm, and the total height of the isolator after bonding, h, was 20.0 mm.

The specimens were manufactured in large pads using a hot vulcanization procedure and subsequently cut to the desired size with a width of 100 mm (R = 5.0) and a length of 60 mm (R = 3.0). The length was selected to maintain lateral stability, whereas the width was selected to exceed the minimum aspect ratio of 3.3 required to maintain contact between the elastomer and the upper and lower supports regardless of rollover. With R = 5.0, B_{max} = 33 %, and bond lengths of B = 0 % and 20 % were considered, for the unbonded (UB) and partially bonded (PB) isolators, respectively.

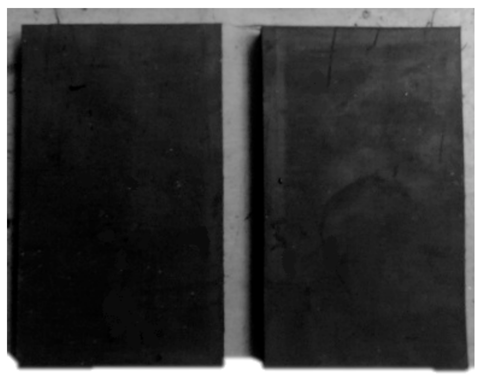

Fig. 5 – FREI specimens prior to partial bonding to the steel end plates

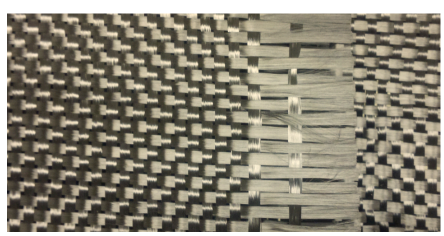

Fig. 6 – Plain weave bi-direction carbon fiber reinforcement

3.2 Experimental Apparatus and Test Procedures

The experimental apparatus, shown in Fig. 7, was constructed with the ability to conduct vertical, cyclic lateral, and rotation tests, individually or in any combination. The vertical load was applied by the two vertical actuators under simultaneous vertical load control and displacement control. The combined control methods achieve the targeted vertical load, while preventing any rotations in order to maintain a level surface. The vertical displacement was measured with four laser transducers positioned at the four corners of the loading platens. The vertical and lateral load was monitored directly with two tri-directional load cells. The lateral displacement was applied with a lateral actuator and measured with a string potentiometer.

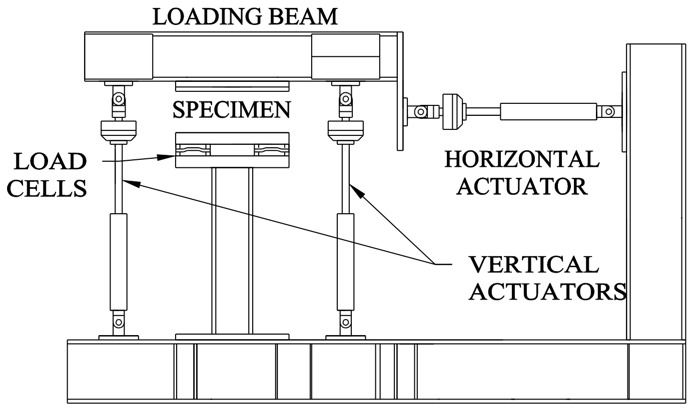

Fig. 7 – Experimental apparatus

The UB isolator was tested under an average vertical compressive stress of 2.0 MPa, based on the total plan area, and the PB isolator was tested with an average vertical tensile stress of 0.1 MPa, based on the bonded area. Vertical tests in compression and tension were conducted following the procedure recommended in ISO 22762 [28]. The isolator was monotonically loaded up to the design stress over 10 s and the load held constant for 5 s followed by three sinusoidal cycles with a frequency of 0.2 Hz and amplitude of ±20 % the design stress. The isolator was then monotonically unloaded and visually inspected for damage.

Lateral cyclic tests consisted of five displacement amplitudes in ascending order with u/t_r = 0.25, 0.50, 0.75, 1.00 and 1.50. The isolator was monotonically loaded to the targeted vertical stress. Three fully reversed sinusoidal cycles were conducted at each displacement amplitude with a constant rate of 76.2 mm/s. The isolator was then monotonically unloaded and visually inspect for damage. Only the results of the lateral cyclic tests are presented in this paper.

4. Results

4.1 Effective Lateral Stiffness

The effective lateral stiffness, k_{eff}, was determined from the experimental hysteresis loops as:

$$k_{eff} = \frac{F_{\max} - F_{\min}}{u_{\max} - u_{\min}} \tag{2}$$

where F_{max} and F_{min} and u_{max} and u_{min} are the maximum and minimum force and displacement over a fully reversed cycle, respectively. The following discussion corresponds to the first cycle at each displacement amplitude considered.

Figure 8 compares the first cycle hysteresis loops of the PB and UB isolator. Figure 9 shows k_{eff} as a function of u/t_r for the UB and PB isolator. Both isolators demonstrate the characteristic softening expected from an unbonded FREI. By u/t_r = 0.75, k_{eff} has decreased by 25 % and 32 % in the UB and PB isolator, respectively, from the u/t_r = 0.25 cycle. By u/t_r = 1.50, the decrease in k_{eff} increases to 37 % and 48 %, respectively. The PB isolator, tested under a nominal tensile load, had a lower k_{eff} over the entire range considered, and was found to soften more than the UB isolator tested under compression. The PB isolator was initially 15 % softer than the UB isolator; this increased with increasing u/t_r to 29 % at u/t_r = 1.50.

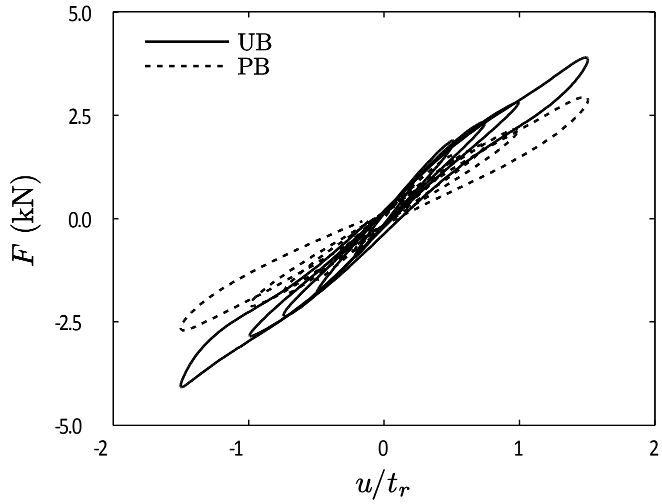

Fig. 8 – Hysteresis loops of the PB and UB isolator

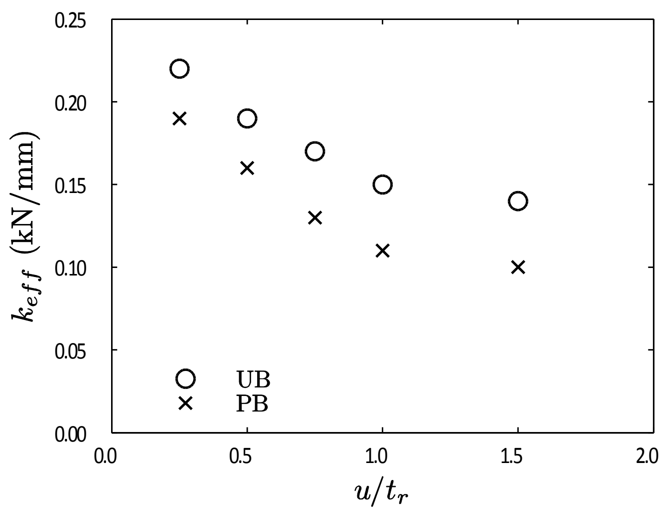

Fig. 9 – Effective lateral stiffness as a function of normalized displacement

The lower value of k_{eff} in the PB isolator with a nominal tensile load is consistent with the findings in the finite element investigation conducted by Van Engelen et al. [5]. Van Engelen et al. [5] used finite element to compare a PB isolator with B = 50 % and 0.2 MPa average tensile stress based on the total plan area, to an UB isolator with 2.0 MPa average compressive stress. The shear forces initially can only be transferred through the partial bond, as shown in Fig. 10(a). Thus, the PB isolator will initially be softer due to the smaller shear area. As the displacement increases, the unbonded sections of the isolator rotate, and are forced into the upper and lower supports as shown in Fig. 10(b). The rotation develops a localized compressive force as contact occurs due to the rotation, which allows the transfer of lateral shear forces due to friction.

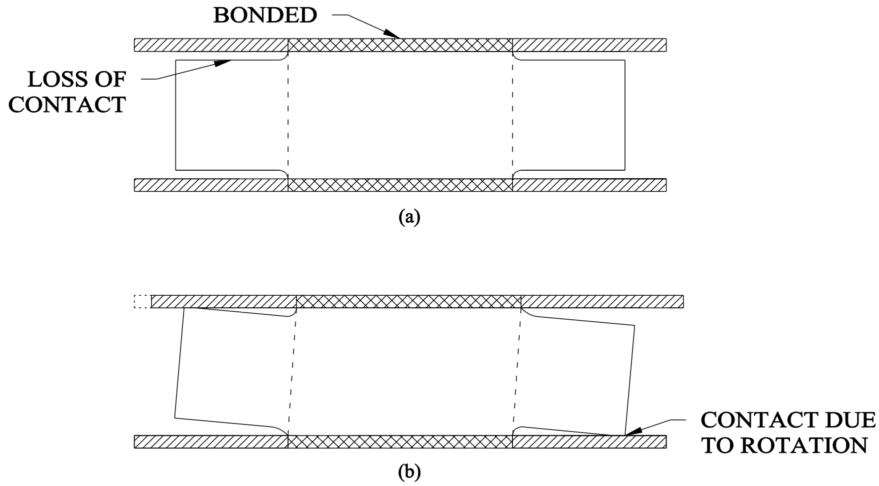

Fig. 10 – An exaggerated deformed PB-FREI (a) under pure vertical tension showing the loss of contact of the unbonded section and (b) under combined lateral displacement and vertical tension showing contact due to rotation of the unbonded section.

4.2 Equivalent Viscous Damping

The equivalent viscous damping, ζ, was calculated as:

$$\zeta = \frac{2W_d}{\pi k_{eff}\left(u_{\max} + |u_{\min}|\right)^2} \tag{3}$$

where W_d is the area enclosed by the hysteresis loops.

Figure 11 compares ζ as a function of u/t_r for the PB and UB isolators. Both the UB and PB isolators display a similar trend. The damping initially decreases to a minimum, and then increases over the u/t_r = 1.50 cycle. The damping in the PB isolator was consistently higher than the UB isolator by approximately 5-23%, depending on the displacement amplitude. It was found that the area enclosed by the hysteresis loops in the UB case was consistently larger than the PB case. Therefore, the larger value of ζ can be attributed to the lower value of k_{eff} in the PB isolator, as discussed in the previous section.

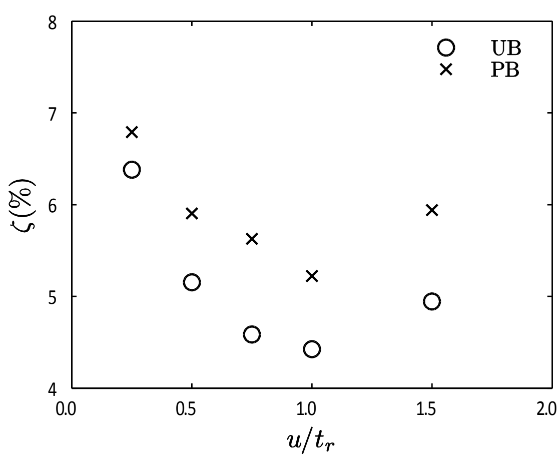

Fig. 11 – Equivalent viscous damping as a function of lateral displacement

5. Conclusions

This paper experimentally investigated a PB-FREI under combined vertical tensile loads and lateral displacement. PB-FREIs are a hybrid of unbonded FREIs and fully bonded FREIs with the intention of addressing concerns over the potential for slip and residual displacements in certain loading conditions, and vertical tensile load resistance.

This paper serves as a proof-of-concept. The PB-FREI considered, tested with a nominal tensile load, demonstrated a similar lateral softening and stiffening response as the control unbonded FREI specimen, tested in compression. The lateral softening and stiffening response is the characteristic feature of stable unbonded FREIs. The partial bond and tensile load did not compromise this response, or result in a lateral instability. It was found that the PB-FREI was consistently softer, and achieved higher damping than the unbonded FREI. These results are consistent with earlier finite element investigations conducted on PB-FREIs. The partial bond prevents slip, and has been shown to successfully transfer a nominal tensile load.

This experimental program is part of a larger on-going investigation being conducted on PB-FREIs with a nominal vertical tensile load. It is expected that this research will further reinforce the above conclusions.

6. Acknowledgements

Financial support for this study was provided by the McMaster University Centre for Effective Design of Structures (CEDS) funded through the Ontario Research and Development Challenge Fund (ORDCF) as well as an Early Researcher Award (ERA) grant, both of which are programs of the Ministry of Research and Innovation (MRI).

7. References

[1] Kelly JM, Konstantinidis D (2011): *Mechanics of Rubber Bearings for Seismic and Vibration Isolation*. Chichester UK: John Wiley & Sons.

[2] Kelly JM (1999): Analysis of fiber-reinforced elastomeric isolators. *Journal of Seismology and Earthquake Engineering,* **2** (1), 19-34.

[3] Toopchi-Nezhad H, Tait MJ, Drysdale RG (2008): Testing and modeling of square carbon fiber-reinforced elastomeric seismic isolators. *Structural Control and Health Monitoring*, **15**, 876-900.

[4] Toopchi-Nezhad H, Drysdale RG, Tait MJ (2009): Parametric study on the response of stable unbonded-fiber reinforced elastomeric isolators (SU-FREIs). *Journal of Composite Materials,* **43** (15), 1569-1587.

[5] Van Engelen NC, Osgooei PM, Tait MJ, Konstantinidis D (2015): Partially bonded fiber-reinforced elastomeric isolators (PB-FREIs). *Structural Control and Health Monitoring,* **22** (3), 417-432.

[6] Kelly JM, Takhirov SM (2002): Analytical and experimental study of fiber-reinforced strip isolators. *Technical Report PEER 2002/11*, Pacific Earthquake Engineering Research Center, Berkeley, USA.

[7] Kelly JM, Calabrese A (2013): Analysis of fiber-reinforced elastomeric isolators including stretching of reinforcement and compressibility of elastomer. *Ingegneria Sismica*, **30** (3), 5-16.

[8] Angeli P, Russo G, Paschini A (2013): Carbon Fiber-reinforced rectangular isolators with compressible elastomer: analytical solution for compression and bending. *International Journal of Solids and Structures,* **50** (22), 3519-3527.

[9] Kelly JM, Van Engelen, NC (2015): Single series solution for the rectangular fiber-reinforced elastomeric isolator compression modulus. *Technical Report PEER 2015/03*. Pacific Earthquake Engineering Research Center, Berkeley, USA.

[10] Pinarbasi S, Okay F (2011): Compression of hollow-circular fiber-reinforced rubber bearings. *Structural Engineering and Mechanics,* **38** (3), 361-384.

[11] Kelly JM, Van Engelen NC (2016): Fiber-reinforced elastomeric bearings for vibration isolation. *Journal of Vibration and Acoustics,* **138** (1), 011015.

[12] Hedayati Dezfuli F, MS Alam (2014): Performance of carbon fiber-reinforced elastomeric isolators manufactured in a simplified process: experimental investigations. *Structural Control and Health Monitoring,* **21** (11), 1347-1359.

[13] Strauss A, Apostolidi E, Zimmermann T, Gerhaher U, Dritsos S (2014): Experimental investigations of fiber and steel reinforced elastomeric bearings: shear modulus and damping coefficient. *Engineering Structures,* **75**, 402-413.

[14] Karimzadeh Naghshineh A, Akyuz U, Caner A (2014): Comparison of fundamental properties of new types of fiber-mesh-reinforced seismic isolators with conventional isolators. *Earthquake Engineering and Structural Dynamics,* **43**, 301-316.

[15] Moon BY, Kang GJ, Kang BS, Kim GS, Kelly JM (2003): Mechanical properties of seismic isolation system with fiber-reinforced bearing of strip type. *International applied mechanics*, **39** (10), 1231-1239.

[16] Toopchi-Nezhad H, Tait MJ, Drysdale, RG (2008): Lateral response evaluation of fiber-reinforced neoprene seismic isolators utilized in an unbonded application. *Journal of Structural Engineering*, **134** (10), 1627-1637.

[17] Toopchi-Nezhad H, Drysdale RG, Tait MJ (2009): Parametric study on the response of stable unbonded-fiber reinforced elastomeric isolators (SU-FREIs). *Journal of Composite Materials,* **43** (15), 1569-1587.

[18] Toopchi-Nezhad H, Tait MJ, Drysdale RG (2009): Shake table study on an ordinary low-rise building seismically isolated with SU-FREIs (Stable Unbonded-Fiber Reinforced Elastomeric Isolators). *Earthquake Engineering and Structural Dynamics,* **38**, 1335-1357.

[19] Russo G, Pauletta M, Cortesia A (2013): A study on experimental shear behavior of fiber-reinforced elastomeric isolators with various fiber layouts, elastomers and aging conditions. *Engineering Structures*, **52**, 422–433.

[20] Das A, Dutta A, Deb SK (2014): Performance of fiber-reinforced elastomeric base isolators under cyclic excitation. *Structural Control and Health Monitoring,* **22** (2), 197-220.

[21] Toopchi-Nezhad H, Tait MJ, Drysdale RG (2011): Bonded versus unbonded strip fiber reinforced elastomeric isolators: finite element analysis. *Composite Structures*, **93**, 850-859.

[22] Moon BY, Kang GJ, Kang BS, Kelly JM (2002): Design and manufacturing of fiber reinforced elastomeric isolator for seismic isolation. *Journal of Materials Processing Technology*, **130-131**, 145-150.

[23] Van Engelen NC, Tait MJ, Konstantinidis D (2014): Model of the shear behavior of unbonded fiber-reinforced elastomeric isolators. *Journal of Structural Engineering* **141** (7), 04014169.

[24] Kelly JM, Konstantinidis D (2007): Low-cost seismic isolators for housing in highly-seismic developing countries. *ASSISi 10th World Conference on Seismic Isolation, Energy Dissipation and Active Vibrations Control of Structures*, Istanbul, Turkey.

[25] Kelly JM (2003): Tension buckling in multilayer elastomeric bearings. *Journal of Engineering Mechanics,* **129** (12), 1363-1368.

[26] Foster BAD (2011): Base isolation using stable unbonded fibre reinforced elastomeric isolators (SU-FREIs). *M.A.Sc. thesis*, McMaster University, Hamilton, Canada.

[27] Kumar M, Whittaker AS, Constantinou MC (2015): Experimental investigation of cavitation in elastomeric seismic isolation bearings. *Engineering Structures*, **101**, 290-305.

[28] ISO (2010): Elastomeric seismic-protection isolators. *ISO 22762*, ISO, Geneva, Switzerland.